

# Controlled Undercooling of Liquid Nickel in Contact with ZrO<sub>2</sub> and Al<sub>2</sub>O<sub>3</sub> Substrates under Varying Oxygen Partial Pressures

MARTIN E. VALDEZ, PELLO URANGA, and ALAN W. CRAMB

The undercooling of a liquid metal, when it is in contact with a particular oxide surface that is a heterogeneous nucleant for solidification, can be measured by observing the recalescence of a sessile droplet in contact with substrates of different compositions under controlled oxygen partial pressures. In this work, the undercooling of pure liquid nickel sessile droplets in contact with ZrO<sub>2</sub> and Al<sub>2</sub>O<sub>3</sub> substrates was measured. The undercooling of pure nickel was affected by the oxygen partial pressure in the surrounding gas phase and exhibited a maximum undercooling of 320 °C for an Al<sub>2</sub>O<sub>3</sub> substrate and 316 °C for a ZrO<sub>2</sub> substrate, both at a PO<sub>2</sub> close to 10<sup>-19</sup> atm. The undercooling of nickel decreases for lower oxygen partial pressures to an average close to 200 °C and for higher oxygen partial pressures to values below 150 °C. The experimental results were compared with the undercooling of iron droplets, and the effect of the substrate orientation on nucleation was also measured.

DOI: 10.1007/s11663-006-9018-x

© The Minerals, Metals & Materials Society and ASM International 2007

## I. INTRODUCTION

THE degree of undercooling, the difference in temperature between the equilibrium melting point in pure materials or the liquidus in alloys and the actual temperature at which solidification initiates, generally depends on the availability of sites where nucleation can occur heterogeneously. If such surfaces are absent, the measured undercooling is a maximum and corresponds to homogeneous nucleation. The value of undercooling for homogeneous nucleation should be a property of a pure metal, because it depends on the thermodynamics of solidification and the liquid-solid surface energy, according to the classical view. Any undercooling measured for a given metal, that is different from the homogeneous nucleation undercooling for the pure material, can be attributed to two factors: a change in the metal composition and the presence of pre-existing solid-liquid or liquid-liquid interfaces. If the metal composition changes, the undercooling can increase or decrease depending on the specific effect of the alloying element. If a number of solid particles that can act as heterogeneous nucleation sites are present, the undercooling should decrease from that of homogeneous nucleation. The presence of solids implies the presence of dissolved species in the liquid metal, and recently it was

shown that varying the oxygen content of liquid iron in contact with alumina could change the measured undercooling. Thus, accurate measurement of undercooling in a heterogeneous-nucleation situation in a liquid metal requires the control of the surfaces available for nucleation and the chemistry of the melt. Table I shows some undercooling measurements for Ni alloys using different techniques.

Turnbull and co-workers<sup>[2]</sup> pioneered a technique for measuring homogeneous nucleation by measuring the maximum undercooling of a large number of small droplets. The maximum undercooling measured for iron under these conditions was 295 °C and the maximum value measured for nickel was 319 °C, as shown in Table I.

As an example of the effect of metal composition, Kudoh and Jones suggested that oxygen might affect the degree of undercooling,<sup>[5]</sup> while the effect of impurities was shown by differential scanning calorimetry experiments by Mizoguchi,<sup>[3]</sup> who measured the undercooling of pure nickel and Fe-Ni alloys containing TiN, Al<sub>2</sub>O<sub>3</sub>, and Ti<sub>2</sub>O<sub>3</sub> particles.

Our experimental approach to study the factors that define the undercooling of a given metal/oxide couple was to measure the undercooling of pure iron droplets in contact with Al<sub>2</sub>O<sub>3</sub>, ZrO<sub>2</sub>, and MgO substrates under controlled oxygen partial pressures in a sessile drop experiment.<sup>[7,8]</sup> The experimental results for iron showed that the undercooling is not unique but is affected by the oxygen content (Figure 1).

For intermediate oxygen partial pressures, the undercooling of iron on Al<sub>2</sub>O<sub>3</sub> and ZrO<sub>2</sub> substrates was around 290 °C but remained below 150 °C for the less stable MgO. At low oxygen partial pressures, substrate decomposition might be the cause for the observed drop in the undercooling of iron in Al<sub>2</sub>O<sub>3</sub> and ZrO<sub>2</sub> substrates to below 100 °C. The minimum oxygen partial pressure under which deep undercoolings were measured is

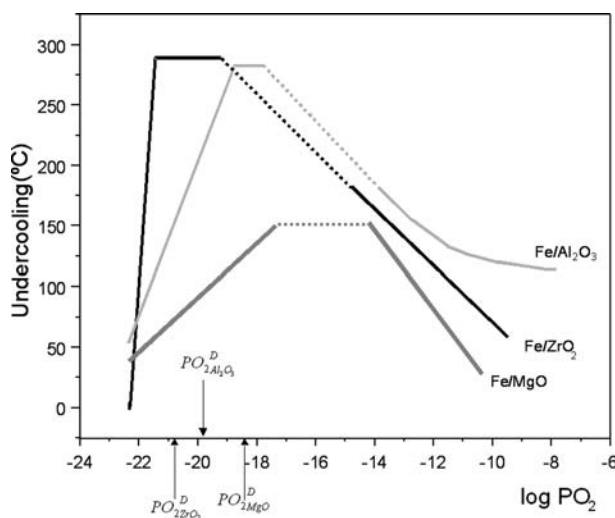
MARTIN E. VALDEZ, Graduate Student and Postdoctoral Fellow, formerly with the Department of Materials Science and Engineering, Carnegie Mellon University, Pittsburgh, PA 15213 is Senior Researcher with the Tenaris Center for Industrial Research, Campana B2804MHA, Argentina. Contact e-mail: mavaldez@tenaris.com. PELLO URANGA, Researcher, is with CEIT and TECNUM, University of Navarra, E-20018 Conostia-San Sebastian, Basque County, Spain. ALAN W. CRAMB, formerly Professor with the Department of Materials Science, Carnegie Mellon University, is Dean of Engineering, Rensselaer Polytechnic Institute, Troy, NY 12180.

Manuscript submitted April 3, 2006.

Article published online April 19, 2007.

**Table I. Undercooling Measurements for Ni Alloys\***

Author	Ref.	Material	Method	$\Delta T^*$		
Ward	1	Ni	levitation	365		
Turnbull	2	Ni	small droplets on quartz or Pyrex	319		
Walker	1	Ni	encasing 400 to 500 g	285		
Mizoguchi	3	Ni	DTA—Ar and $\text{Al}_2\text{O}_3$ crucibles	184		
Kudoh	4	Ni	fused silica crucible	152		
Kudoh	5	$\text{Ni-O}$	static undercooling	60–0		
Kudoh	4	Ni	alumina crucible	55		
Jones <i>et al.</i>	6	$\text{Ni-O}$	silica crucible with slag	271–51		
Mizoguchi	3	Fe-Ni : 0 to 6 pct	DTA $\text{Al}_2\text{O}_3$ crucible	TiN catalyst	13	
		Fe-Ni : 6 to 29 pct			68	
		Fe-Ni : 0 to 9 pct			$\text{Al}_2\text{O}_3$ catalyst	36 to 40

\*Maximum  $\Delta T$  observed.Fig. 1—Schematic of the undercooling of pure iron on  $\text{ZrO}_2$ ,  $\text{Al}_2\text{O}_3$ , and  $\text{MgO}$  as a function of  $\text{PO}_2$ .

similar to the oxygen partial pressure for substrate decomposition at the soaking temperature ( $\text{PO}_2^D$  in Figure 1). The effect of substrate decomposition on undercooling was verified by measuring the undercooling of Fe-Al samples using a differential thermal analyzer (DTA).<sup>[7]</sup> In the DTA experiments, the decrease in aluminum content by vaporization was detected as an increase in the melting temperature of the sample; and this decrease in aluminum was accompanied by an increase in the undercooling. It was concluded that the decrease in undercooling for low oxygen partial pressure could be caused by the increasing aluminum content associated with  $\text{Al}_2\text{O}_3$  decomposition.

The undercooling of iron also decreased for increasing oxygen partial pressure as verified when the gas was changed from gettered Ar/Ar-H<sub>2</sub> to CO/CO<sub>2</sub> mixtures.

In Figure 1, it can be observed that the maximum undercooling was the same for different stable substrates (such as  $\text{Al}_2\text{O}_3$  and  $\text{ZrO}_2$ ); the results also showed that the undercooling increased as the wettability decreased and that the maximum undercooling was similar to the values reported previously as homogeneous nucleation

undercooling. All of these observations suggest that homogeneous nucleation of the metal is possible even when a heterogeneous nucleation surface is clearly available. Due to the fact that the homogeneous undercooling is a property of the metal and not of the substrate, the maximum undercooling should be different for other metals. In order to look into the effect of the “metal” used on the undercooling, the sessile drop experiments were repeated using pure Ni.

## II. EXPERIMENTAL

The experimental approach of this work consisted of measuring the undercooling of pure nickel droplets (0.25 g) on top of oxide substrates, using a sessile drop setup. The sessile drop technique is usually used to measure the contact angle of liquid metals in contact with substrates and the surface tension of liquid metals, but in this case, it also provides the undercooling by detecting droplet recalescence during cooling. The detailed experimental apparatus and the oxygen control setup have been discussed previously.<sup>[7,8]</sup> In this work, the soaking temperature was 1500 °C for the nickel experiments and 1600 °C in the combined experiments (Fe and Ni). Table II describes the materials employed in the experiments and Table III the substrates.

The cross section of the furnace showing the setup for an experiment in which the undercoolings of Ni and Fe are compared is shown in Figure 2.

**Table II. Pure Metals Composition**

Material	Composition
Pure iron	Fe: 99.995 pct
Pure Ni	Ni: 99.999 pct, Al: 0.001 pct

**Table III. Substrate Composition and Orientation**

Material	Company	Orientation
$\text{Al}_2\text{O}_3$	Vesuvius	polycrystalline
$\text{ZrO}_2$	Crystal	110 111

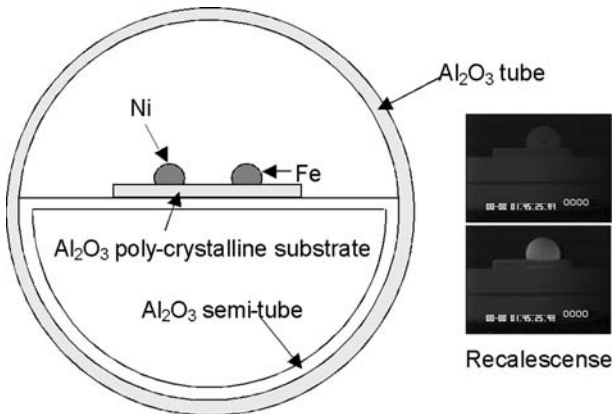


Fig. 2—Experimental setup for undercooling of Fe and Ni on  $\text{Al}_2\text{O}_3$  polycrystalline.

The samples were repeatedly melted and solidified by heating at  $3\text{ }^{\circ}\text{C}/\text{min}$ , soaking for 1 h, and cooling again at  $3\text{ }^{\circ}\text{C}/\text{min}$ . The cooling cycle was recorded in super VHS and recalcense was detected due to the increase in brightness of the droplet (insert in Figure 2). The difference between the temperature of the droplet and the furnace temperature was calibrated by melting pure metals. The undercooling is the difference between the melting temperature of the pure metal and the temperature of the droplet when the increase in brightness is detected.

### III. RESULTS

#### A. Undercooling of Nickel on $\text{Al}_2\text{O}_3$ Substrates

A multiple recalcense experiment was performed in which a droplet of pure Fe and a droplet of pure Ni were placed in the furnace on top of the same  $\text{Al}_2\text{O}_3$  substrate (as shown in Figure 2). The comparison of the results for Fe and Ni is shown in Figure 3. The line connecting the Fe and Ni points represents the fact that both undercoolings were measured in the same experiment.

Figure 3 shows that the undercooling of Fe is much more sensitive to changes in the oxygen partial pressure than nickel. As observed in previous works<sup>[7,8]</sup> (Figure 1), in extremely low oxygen partial pressure, a drop in the undercooling of pure iron was observed; this was also observed but in a lesser degree for Ni. This experiment was useful to verify the phenomena previously measured for Fe and to detect a different behavior in the case of the Ni droplets.

The next set of experiments was performed by placing only a nickel droplet on alumina polycrystalline substrates. Figure 4 shows the relationship between undercooling and the oxygen partial pressure for experiments carried out under an Ar-5 pct H<sub>2</sub> gas mixture, ultra-high-purity argon, and CO/CO<sub>2</sub> mixtures. The error bars indicate that the PO<sub>2</sub> changed during cooling. The maximum PO<sub>2</sub> corresponds to the setup by the CO/CO<sub>2</sub> ratio at the soaking temperature, while the minimum value corresponds to the value setup by the CO/CO<sub>2</sub> ratio at the solidification temperature.

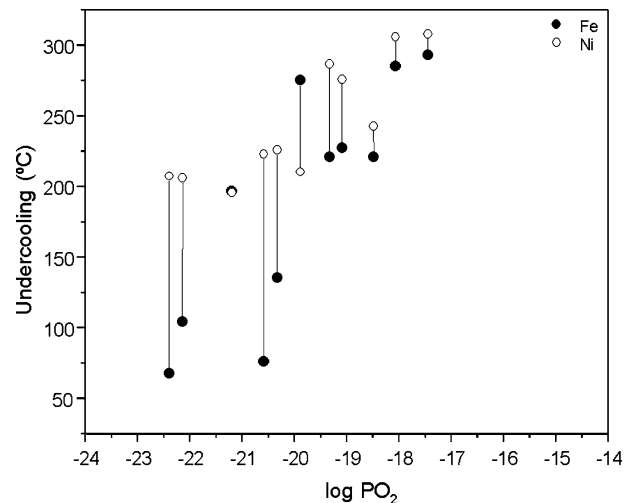


Fig. 3—Comparison between the recalcense of Fe and Ni droplets measured simultaneously in an  $\text{Al}_2\text{O}_3$  substrate.

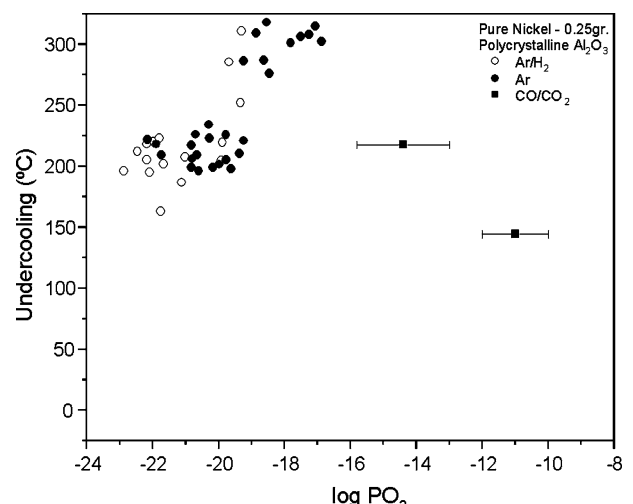


Fig. 4—Undercooling of Ni on  $\text{Al}_2\text{O}_3$  for Ar and Ar-H<sub>2</sub> experiment and CO/CO<sub>2</sub> mixtures.

The results under Ar and Ar-H<sub>2</sub> indicated two different stages. The first stage, for oxygen partial pressures below  $10^{-20}$  atm, with an average undercooling of  $210\text{ }^{\circ}\text{C}$ ; and the second stage, for oxygen partial pressures higher than  $10^{-20}$  atm, with an average undercooling of  $280\text{ }^{\circ}\text{C}$ . The transition between both stages was observed for both Ar-H<sub>2</sub> and Ar atmospheres showing that the results are the same independently of the gas type but not of the oxygen partial pressure. The difference between both stages was statistically checked with a 0.05 confidence level. These undercooling values are comparable to the maximum values reported by other authors in Table I. The maximum undercooling measured for Ni was  $320\text{ }^{\circ}\text{C}$  and is close to the value of  $319\text{ }^{\circ}\text{C}$  reported by Turnbull<sup>[2]</sup> under a He atmosphere and Pyrex flux. Jones and Weston<sup>[6]</sup> measured values above  $200\text{ }^{\circ}\text{C}$  for “low oxygen melts.”

Even though the increase in undercooling was observed during multirecalcense experiments, the maximum undercooling can be achieved in a single

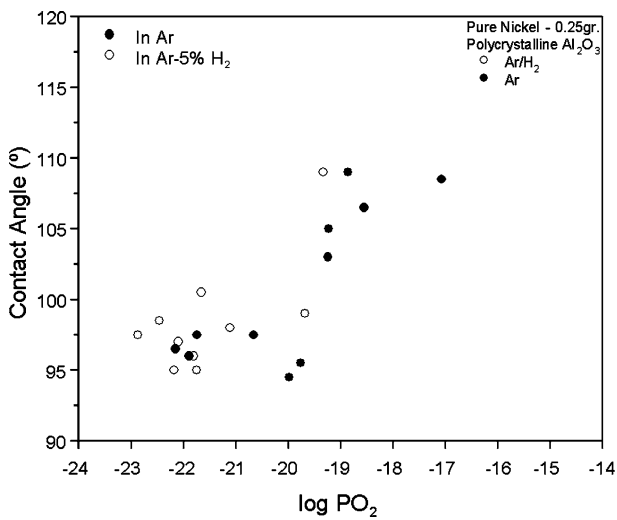


Fig. 5—Contact angle vs  $\text{PO}_2$  for Ni on  $\text{Al}_2\text{O}_3$  polycrystalline substrate.

experiment if the  $\text{PO}_2$  is set up in the correct range. A single recalescence experiment was performed under a  $\text{PO}_2$  of  $10^{-19.6}$  atm with an undercooling of  $314.5^\circ\text{C}$ .

The drop in undercooling observed in the Fe experiments for increasing oxygen partial pressures (Figure 1) was also observed in the CO/CO<sub>2</sub> experiments for nickel (Figure 4).

Figure 5 shows the change in contact angle with oxygen partial pressure. The two stages observed for the undercooling (Figure 4), with a transition around  $10^{-20}$  atm, were also observed in the contact angle. For the lowest oxygen levels, an average angle of about 97 deg was measured. For oxygen partial pressures higher than  $10^{-20}$ , the average contact angle increased up to 107 deg.

The measurement of the contact angle in the CO/CO<sub>2</sub> experiments was not reliable due to pinning caused by  $\text{Al}_2\text{O}_3$  formation.

The difference in contact angle between both ranges can be clearly appreciated in Figure 6. Figure 6(a) corresponds to a low  $\text{PO}_2$  range ( $\log \text{PO}_2 = -22.87$ ) with a contact angle of 97.5 deg, and Figure 6(b) to a higher  $\text{PO}_2$  level ( $\log \text{PO}_2 = -19.24$ ) and a contact angle of 103 deg.

Ogino<sup>[9]</sup> measured the contact angle of liquid nickel on  $\text{Al}_2\text{O}_3$  under Ar-H<sub>2</sub>O-H<sub>2</sub> gas mixtures at  $1600^\circ\text{C}$  and studied the effect of oxygen content by analyzing the oxygen in the droplets after cooling. In Ogino's work, a maximum contact angle, greater than 120 deg, was observed for intermediate oxygen content. The angle was observed to decrease to about 115 deg as the oxygen content increases and also to as low as 100 deg as the oxygen decreases. Ogino attributed the decrease for low oxygen to the effect of  $\text{Al}_2\text{O}_3$  dissociation.<sup>[9]</sup>

#### B. Analysis of the $\text{Ni}/\text{Al}_2\text{O}_3$ Samples after the Experiments

The top view of a nickel droplet is shown under the SEM in Figure 7. The shaded areas that can be observed in the picture were found to be  $\text{Al}_2\text{O}_3$ . The oxygen partial pressure in the case of this particular droplet was below  $10^{-21}$  atm during the entire cycle.

The presence of alumina in the samples that were melted under low oxygen partial pressure conditions was also observed in the case of the iron experiments.<sup>[7]</sup> This indicates that at these extremely low oxygen contents, the substrate dissolves into the metal. This type of interaction between the droplet and substrate can be confirmed by analyzing the surface of the substrate in an area where the droplet has seated during the experiment.

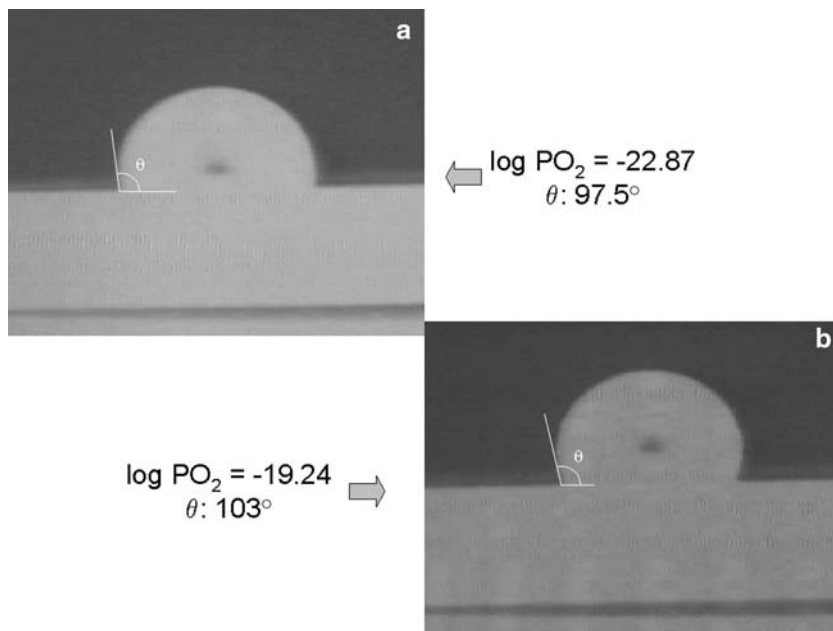


Fig. 6—Profiles of liquid Ni droplets at  $1500^\circ\text{C}$ : (a) lower  $\text{PO}_2$  range and (b) higher  $\text{PO}_2$  range.

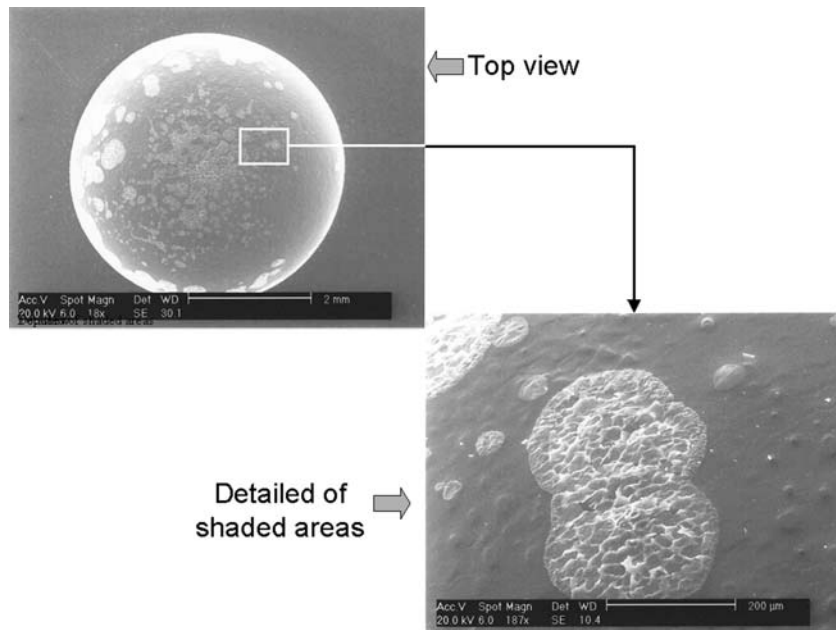


Fig. 7—Droplet surface after recalescence and cooling cycle.

This is made possible in those experiments in which the liquid droplet moves. In the SEM picture on Figure 8, an area of the substrate where the droplet seated (Figures 8(c) and (d)) and an area of the substrate where the droplet did not seat (Figure 8(a)) are compared. Figure 8(b) indicates the location relative to the droplet, from where Pictures 8(d) and 8(a) were taken. Figure 8(d) shows dendritic  $\text{Al}_2\text{O}_3$  that has nucleated on the substrate surface probably due to an increase in the oxygen or a decrease in temperature. This dendritic  $\text{Al}_2\text{O}_3$  was not observed in the areas of the substrates that were not wetted by the Ni droplet (Figure 8(a)).

The analysis of the cross-sectional interface of the Ni/ $\text{Al}_2\text{O}_3$  sample after the CO-CO<sub>2</sub> experiments shows no reaction layer.

### C. Undercooling of Nickel on $\text{ZrO}_2$ Substrates

A series of almost 50 undercooling experiments of nickel was carried out using two single-crystal-zirconia substrates of (110) and (111) orientation parallel to the surface. The range of oxygen partial pressure covered was  $10^{-23.5}$  to  $10^{-18.2}$  atm using Ar-H<sub>2</sub> and gettered Ar, and up to  $10^{-9}$  atm using CO-CO<sub>2</sub> mixtures. It was

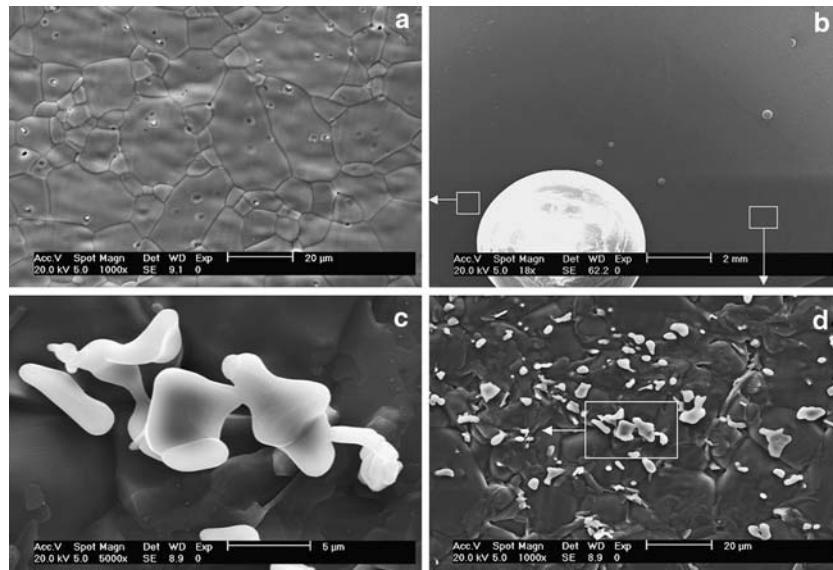


Fig. 8—Modification of the substrate by the Ni droplet: (a) substrate surface in an area where the Ni droplet has not seated, (b) top view of the Ni droplet after experiment, (c) detail of dendrites, and (d) substrate surface in an area where the Ni droplet has seated.

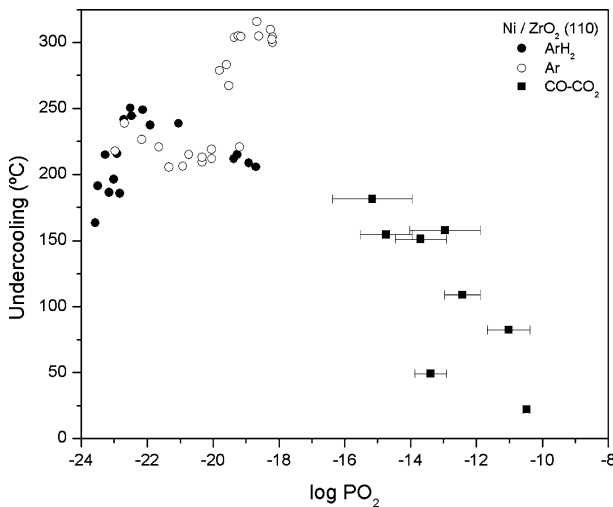


Fig. 9—Change in undercooling with  $\text{PO}_2$  for nickel on two different zirconia single-crystal substrates corresponding to (110) (Ar,  $\text{Ar-H}_2$ ,  $\text{CO-CO}_2$ ).

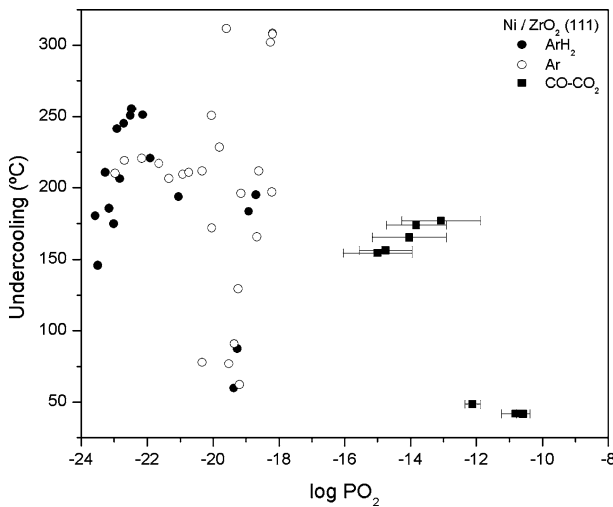


Fig. 10—Change in undercooling with  $\text{PO}_2$  for nickel on two different zirconia single-crystal substrates corresponding to (111) (Ar,  $\text{Ar-H}_2$ ,  $\text{CO-CO}_2$ ).

verified by X-ray that the bulk orientation of the substrates remains unmodified after the experiments in an area adjacent to the nickel droplet. The results of the undercooling measurements are shown in Figures 9 and 10.

In the low  $\text{PO}_2$  range ( $10^{-23}$  to  $10^{-20.5}$ ) the undercooling of Ni on both substrates was similar to the values measured in  $\text{Al}_2\text{O}_3$  but with more scatter (between 150 °C to 250 °C). In this range of  $\text{PO}_2$ , the undercooling of Ni was the same regardless of the orientation of the  $\text{ZrO}_2$  substrate. For  $\text{PO}_2$  greater than  $10^{-20.5}$  and below  $10^{-17}$ , the undercooling in the (110) substrate increases to a maximum of 316 °C repeating a behavior observed for other systems. On the contrary, the undercooling on  $\text{ZrO}_2$  (111) showed values as high as 311.6 °C and as low as 62 °C. The variation in undercooling is caused by the effect of the oxygen partial

pressure, as was the case for Ni on  $\text{Al}_2\text{O}_3$  and the iron experiments.<sup>[7,8]</sup>

The contact angle did not vary greatly with the  $\text{PO}_2$ . This may be caused by pinning of the droplet. It was observed that in many cases the droplet was not symmetric. The average contact angle between both orientations was not significantly different and the average contact angle was 105.1 deg.

#### D. Analysis of the $\text{Ni/ZrO}_2$ Samples after the Experiments

The  $\text{Ni/ZrO}_2$  droplets were analyzed after the experiments under the SEM. There was no oxidation in the surface of the droplets. Small amounts of a silicon rich phase were detected in the surface of the droplets and also in the interface between the droplet and the substrate. Contamination with silicon is a problem that was also observed in the  $\text{MgO}$  experiments and is due to the presence of impurities in the refractory materials of the furnace.

As mentioned before pinning of the droplet was observed during the experiments. Figure 11 shows SEM pictures of a nickel droplet on  $\text{ZrO}_2$  (110) after experiments under Ar and  $\text{Ar-H}_2$  for a maximum  $\text{PO}_2$  of approximately  $10^{-19}$  atm. Figure 11(a) shows a top view of the droplet. Due to de-wetting or movement of the droplet, an area previously wetted by the liquid Ni can be observed in Figure 11(b) and with more detail in Figures 11(c) and (d). In these pictures, it can be observed that the substrate dissolves into the metal in a preferential way, giving rise to the formation of porosity. It can also be observed that the rim of the droplet is defined by a number of “peaks” that may act as pinning points.

## IV. DISCUSSION

The main observation of the nickel experiments presented above is that, as observed for the case of the iron experiments, the undercooling of pure nickel also was affected by the oxygen partial pressure.

#### A. Comparison of Fe and Ni

The Ni experiments showed a maximum undercooling of 320 °C for the experiments performed on  $\text{Al}_2\text{O}_3$  substrates and 316 °C for the experiments on  $\text{ZrO}_2$  substrates. This maximum was located at a  $\text{PO}_2$  close to  $10^{-19}$  atm. Figures 12 and 13 compare the undercooling in  $\text{ZrO}_2$  and  $\text{Al}_2\text{O}_3$  for Fe and Ni respectively.

The decrease in undercooling of iron for low oxygen partial pressure is related to the dissolution of the substrate. In the case of the nickel experiments, dissolution of the substrate was verified by the presence of  $\text{Al}_2\text{O}_3$  particles in the  $\text{Ni/Al}_2\text{O}_3$  droplets, both in the metals surface (Figure 7) and on the substrate surface (Figure 8). This evidence is not as strong as in the case of Fe because aluminum is the main impurity of the Ni samples (Table II), so it is difficult to conclude that the only source of aluminum in the metal is the substrate. In

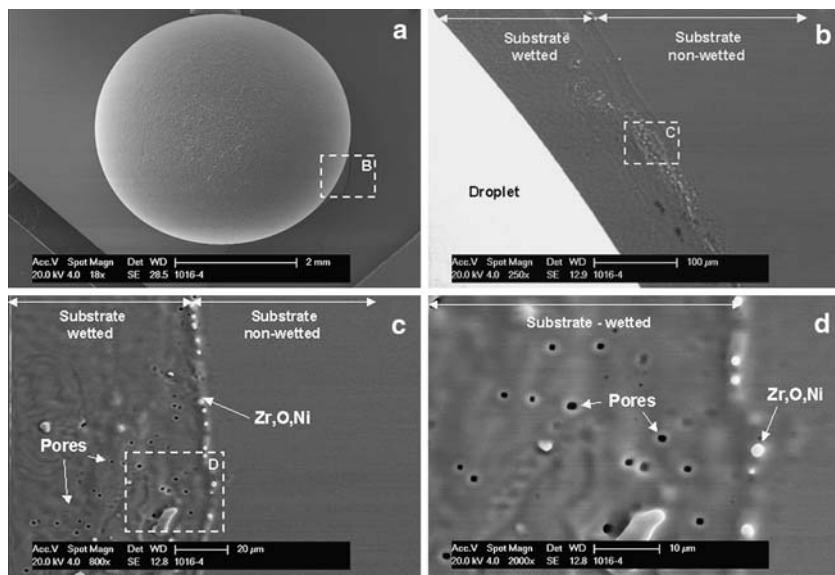


Fig. 11—SEM pictures of a nickel droplet on  $\text{ZrO}_2$  (110) after Ar and  $\text{ArH}_2$  experiments: (a) top view, (b) substrate modification close to the droplet, and (c) and (d) detail of an area wetted by the droplet showing pinning points and pores.

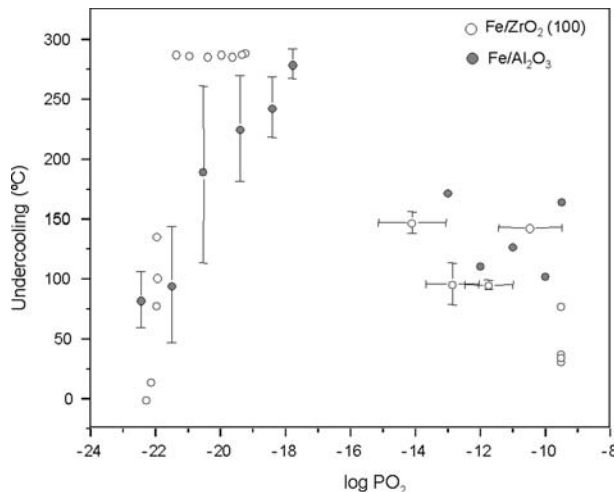


Fig. 12—Comparison of the undercooling of Fe on  $\text{Al}_2\text{O}_3$  and  $\text{ZrO}_2$  (100) substrates.

In the case of the  $\text{ZrO}_2$  experiments, the dissolution of the substrate was evident through the formation of pores in previously wetted areas, as well as a ridge of pinning points. Some authors suggest that these pinning points or ridges are formed through dissolution, transport in the liquid phase, and precipitation,<sup>[10]</sup> making dissolution of the substrate a necessary condition during the experiments. However, even though both metals showed a drop in undercooling, in the case of Ni, the drop was considerably less pronounced (Figures 12 and 13). The fact that the drop occurs at similar oxygen partial pressures for both metals on the same substrate is an indication that this drop may be related to the destabilization of the substrate as hypothesized previously. This is clear for the  $\text{Al}_2\text{O}_3$  experiments but not for the  $\text{ZrO}_2$  experiments. The plateau observed for the

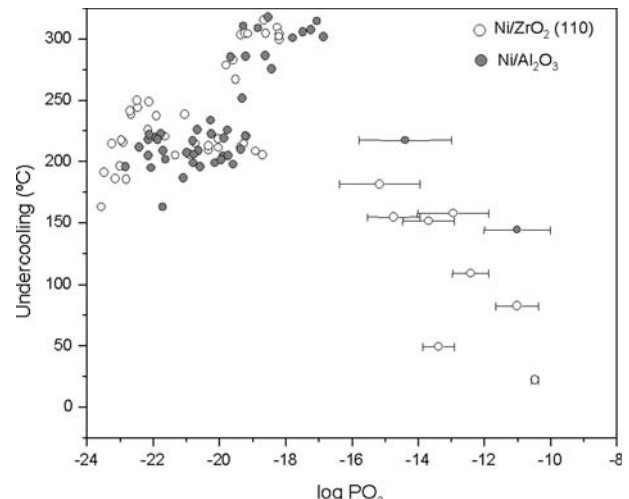


Fig. 13—Comparison of the undercooling of Ni on  $\text{Al}_2\text{O}_3$  and  $\text{ZrO}_2$  (110) substrates.

Fe/ $\text{ZrO}_2$  experiments was not clear in the case of Ni/ $\text{ZrO}_2$ . Overall, the effect of dissolution on the nickel seems to be less pronounced resulting in a moderate drop in undercooling ( $\Delta T > 150$  °C) toward low  $\text{PO}_2$ . The experiments under  $\text{CO}/\text{CO}_2$  showed that the drop in undercooling with increasing oxygen partial pressure is also observed in the case of the Ni experiments. As shown in the figures, the undercooling in  $\text{ZrO}_2$  is slightly lower than in  $\text{Al}_2\text{O}_3$  for both metals.

An interesting point to highlight is the maximum undercooling. The iron experiments published previously<sup>[7,8]</sup> showed that the maximum undercooling was the same for different stable substrates (such as  $\text{Al}_2\text{O}_3$  and  $\text{ZrO}_2$ ), and it was concluded that homogeneous nucleation of the metal is possible even when a heterogeneous nucleation surface is clearly available.

**Table IV. Maximum Undercooling Measured for Fe and Ni**

Element	Turnbull <sup>[2]</sup>	Sessile Drop		
		Al <sub>2</sub> O <sub>3</sub>	ZrO <sub>2</sub>	SiO <sub>2</sub>
Fe	295	288	289	285.6
Ni	319	320	316	—

Because the homogeneous undercooling is a property of the metal and not of the substrate, the maximum undercooling should be different for other metals. This was our starting hypothesis for this article and the driving force to study the undercooling of Ni. The maximum undercooling of Ni was 320 °C for Al<sub>2</sub>O<sub>3</sub> substrates and 316 °C for ZrO<sub>2</sub> and, as shown in Table IV, is also in very close agreement with the value measured by Turnbull<sup>[2]</sup> as homogeneous nucleation.

The conclusion of our previous work was verified by the maximum undercoolings measured in the Ni experiments: even in a condition where a heterogeneous nucleation surface was clearly available, the maximum undercooling was the same as the maximum undercooling reported by Turnbull for homogeneous nucleation.

### B. Effect of Substrate Orientation

It has been suggested that the disregistry or mismatch between nuclei and substrate is an important factor for heterogeneous nucleation.<sup>[11]</sup> The planar disregistries between the substrate and solid lattices can be calculated following Bramfitt's equation (Eq. [1]):

$$\delta = \sum_{i=1}^3 \delta_{(hkl)s}^{(hkl)n} = \left[ \frac{|(d[uvw]_n^i \cos \varpi) - d[uvw]_s^i|}{d[uvw]_n^i} \right] \times 100 \text{ pct} \quad [1]$$

where  $(hkl)_s$  and  $(hkl)_n$  are low-index planes in the solid and nucleant;  $[uvw]_s$  and  $[uvw]_n$  are low-index directions in the  $(hkl)_s$  and  $(hkl)_n$  planes, respectively;  $d[uvw]$  is the spacing along  $[uvw]$ ;  $\varpi$  is the angle between  $[uvw]_s$  and  $[uvw]_n$ ; and  $i$  is one of the three directions of the crystal with minimum index. Bramfitt used this parameter to explain the difference in efficiency as the heterogeneous nucleant of delta ferrite, exhibited by different carbides and nitrides, by measuring the degree of undercooling during solidification. Many researchers had referred to this parameter.<sup>[12,13,14]</sup> Its effect on undercooling was summarized by Grong who claimed that the undercooling necessary for nucleation of δ-iron (111) on Al<sub>2</sub>O<sub>3</sub> (0001) is a little bit greater than 10 °C. This may be the case at a particular oxygen partial pressure, but it can be as high as ~300 °C, as shown in Figure 1. On the other hand, Kudoh *et al.*<sup>[14]</sup> uses the disregistry theory to explain his findings that alumina is a good heterogeneous nucleation catalyst for nickel. However, in this work, we have already shown that undercoolings as high as 320 °C for pure nickel on alumina substrates are possible. This shows that the analysis of Bramfitt's disregistry may be an important tool but not a conclusive one to determine the hetero-

**Table V. Crystallographic Properties of Analyzed Structures**

Materials	Crystal Structure	Lattice Parameter ( $\times 10^{10}$ m)		Linear Coefficient of Expansion ( $10^6 \text{ K}^{-1}$ )
		$a$ (25 °C)	$c$ (25 °C)	
Nickel	fcc	3.52	—	12.96
Alumina	hcp	4.76	12.99	10
Zirconia	fcc	5.09	—	13.5

**Table VI. Planar Disregistries among Ni, Fe, Al<sub>2</sub>O<sub>3</sub>, and ZrO<sub>2</sub> using First Near Neighbors**

Metal	Substrate	Nuclei	Misfit ( $\delta\%$ )
Ni	Al <sub>2</sub> O <sub>3</sub> (0001)	Ni (110)	63
	ZrO <sub>2</sub> (110)	Ni (110)	2.3
	ZrO <sub>2</sub> (111)	Ni (111)	44.6
	ZrO <sub>2</sub> (100)	Ni (100)	44.2

geneous nucleation potential of different oxides. Clearly, the effect of metal composition in undercooling should also be considered.

The crystallographic parameters of Ni, Al<sub>2</sub>O<sub>3</sub>, and ZrO<sub>2</sub> that will define the mismatch presented in Eq. [1] are listed in Table V.<sup>[15]</sup> The calculated disregistries for the systems studied in this article are presented in Table VI. The calculations were done using the software CaRIne Crystallography 3.1.

The calculation of the disregistry requires the selection of two crystallographic planes, one in each material, as well as the relative orientation among them. The values shown in Table VI indicate that zirconia structure has a small (2.3 pct) misfit with solid nickel for the (110) plane of the zirconia and the (110) plane of the nickel. The minimum misfit increases to 44.6 pct if the zirconia orientation is (111). The crystallographic relations between Ni and ZrO<sub>2</sub> are shown in the schematics of Figure 14.

The undercoolings of nickel on ZrO<sub>2</sub> (111) and (110) were presented in Figures 9 and 10. The behavior observed in ZrO<sub>2</sub> (110) was similar to the one observed for Ni in Al<sub>2</sub>O<sub>3</sub> (as shown in Figure 13) and also similar to the general behavior observed for iron on different substrates. On the other hand, the behavior of ZrO<sub>2</sub> (111) presented a high degree of scatter. The difference in the undercooling measured in simultaneous experiments on these two substrates is shown in Figure 15.

Figure 15 shows that for the lower range of oxygen partial pressure ( $10^{-23}$  to  $10^{-20.5}$ ) as well as for the experiments performed under CO/CO<sub>2</sub> ( $\text{PO}_2 > 10^{-15}$  atm), there is no significant difference between both orientations. Both substrates behave differently at  $\text{PO}_2$  between  $10^{-20}$  and  $10^{-19}$  atm.

These results are important for several reasons. First, they show again that the misfit between the solid lattices is not necessarily the only parameter that determines the undercooling. As pointed out in Figure 14, the misfit between Ni and these two substrates is quite different; an undercooling controlled by misfit cannot be

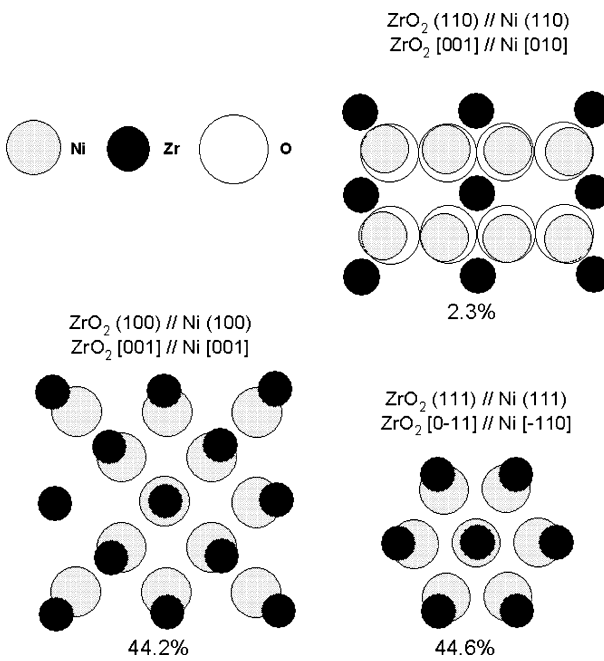


Fig. 14—Crystallographic relationship between zirconia and nickel.

explained by the experimental points in which both substrates show the same undercooling as well as those experiments in which the undercooling of  $\text{ZrO}_2$  (110) was smaller than  $\text{ZrO}_2$  (111). The increase in undercooling for the (110) substrate follows the behavior observed for Ni on  $\text{Al}_2\text{O}_3$ . The different responses of the substrates to the oxygen partial pressure could also be due to the differences in the chemical composition of the surfaces. It is clear from Figure 14 that the  $\text{ZrO}_2$  (110) surface is composed of Zr-O atoms, while the  $\text{ZrO}_2$  (111) surface is either all Zr or all O. Then, the misfit is not the only difference between these two substrates, but it is also the surface composition. The interaction of a metal with different oxygen contents, with these surfaces, can be affected by these compositional differences.

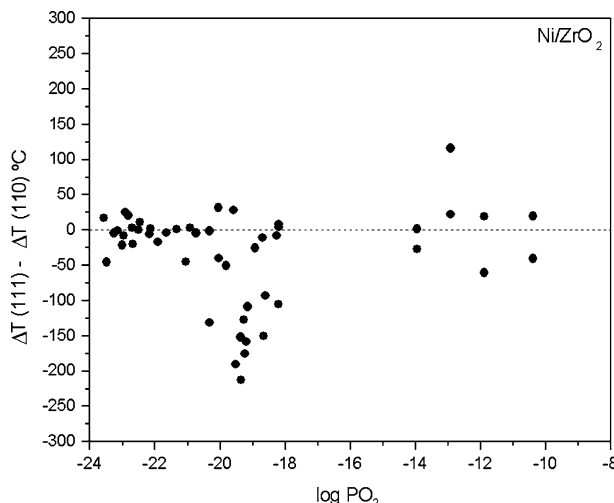


Fig. 15—Difference between undercooling of Ni on  $\text{ZrO}_2$  (111) and (110) substrates as a function of the oxygen partial pressure.

Finally, the results also indicated that even though nucleation is usually described as a process resulting from random fluctuations and of a stochastic nature, this set of experiments indicates that by controlling the oxygen partial pressure, undercooling can be defined quite precisely. Some of the undercoolings for low  $\text{PO}_2$  in Figure 15 are almost equal (for oxygen partial pressures below  $10^{-21}$  atm more than 50 pct of the experiments resulted in a difference of less than 4 pct in the undercooling). In these particular experiments, two droplets placed in two different substrates remain liquid for more than 1 hour and solidified with an average difference in time of one and a half minutes.

## V. CONCLUSIONS

The undercooling of nickel in contact with  $\text{Al}_2\text{O}_3$  polycrystalline substrates and  $\text{ZrO}_2$  single crystals of different orientation was measured under varying oxygen partial pressures. As observed in previous works for iron, the undercooling of pure nickel was also affected by the oxygen partial pressure showing a maximum undercooling of 320 °C for  $\text{Al}_2\text{O}_3$  and 316 °C for  $\text{ZrO}_2$  at a  $\text{PO}_2$  close to  $10^{-19}$  atm. The undercooling of nickel in both substrates decreases for low oxygen partial pressures to an average close to 200 °C and for higher oxygen partial pressures to values below 150 °C.

The comparison of the nickel experiments with the previously reported iron experiments showed that the maximum undercooling of Ni and Fe is similar to the values reported for homogeneous nucleation. This observation is consistent with the fact that the maximum undercooling is independent of the type of substrate but is a function of the type of metal.

The effect of substrate orientation showed either no significant effect in the undercooling or an effect that is not consistent with the minimum lattice misfit criteria. This behavior, together with the effect of oxygen partial pressure, indicates that the misfit is not necessarily the defining parameter that determines undercooling.

## ACKNOWLEDGMENTS

The authors thank the member companies of the Center for Iron and Steelmaking Research, Carnegie Mellon University, and AISI DOE Project No. 0101, "Inclusion Optimization for New Generation Steel Products," for the financial support.

## REFERENCES

- M. Flemings and Y. Shiohara: *Mater. Sci. Eng.*, 1984, vol. 65, pp. 157–70.
- D. Turnbull and R.E. Cech: *J. Appl. Phys.*, 1950, vol. 21, pp. 804–10.
- K. Nakajima, H. Hasegawa, S. Khumkha, and S. Mizoguchi: *Metall. Mater. Trans. B*, 2003, vol. 34B, pp. 539–47.
- A. Abedi, M. Kudoh, and Y. Itoh: *ISIJ Int.*, 1997, vol. 37 (8), pp. 770–75.

5. A. Abedi, M. Kudoh, and Y. Itoh: *ISIJ Int.*, 1995, vol. 35 (6), pp. 589–95.
6. B.L. Jones and G.M. Weston: *J. Aust. Inst. Met.*, 1970, vol. 15 (4), pp. 189–94.
7. M. Valdez, P. Uranga, K. Fuchigami, H. Shibata, and A.W. Cramb: *Metall. Mater. Trans. B*, 2006, vol. 37B (5), pp. 811–21.
8. M. Valdez, H. Shibata, and A.W. Cramb: *Metall. Mater. Trans. B*, 2006, vol. 37B (6), pp. 959–65.
9. K. Ogino and H. Taimatsu: *J. Jpn. Inst. Met.*, 1979, vol. 43 (9), pp. 871–76.
10. E. Saiz, A.P. Tomsia, and R.M. Cannon: *Acta Mater.*, 1998, vol. 46 (7), pp. 2349–61.
11. O. Grong: *Metallurgical Modelling of Welding*, 2nd ed., The Institute of Materials, London, 1997.
12. G.N. Heintze and R. Mc Pherson: *Weld. Res. Suppl.*, 1986, pp. 71s–82s.
13. A. Ostrowski and E.W. Langer: *Scand. J. Metall.*, 1979, vol. 8, pp. 177–84.
14. A. Abedi, M. Kudoh, and Y. Itoh: *ISIJ Int.*, 1997, vol. 37 (8), pp. 770–75.
15. W.B. Pearson: *A Handbook of Lattice Spacings and Structures of Metals and Alloys*, Pergamon Press, New York, NY, 1958, pp. 67–70.